Global NEST Journal, Vol 16, No 3, pp 485-498, 2014

NANOCRYSTALLINE TiO_2 AND HALLOYSITE CLAY MINERAL COMPOSITE FILMS PREPARED BY SOL-GEL METHOD: SYNERGISTIC EFFECT AND THE CASE OF SILVER MODIFICATION TO THE PHOTOCATALYTIC DEGRADATION OF BASIC BLUE- 41 AZO DYE IN WATER

RAPSOMANIKIS A.[1]
PAPOULIS D.[2]
PANAGIOTARAS D.[3]
KAPLANI E.[3]
STATHATOS E.[1,*]

[1]*Electrical Engineering Department*
Technological-Educational Institute of Western Greece
26334 Patras, Greece
[2]*Department of Geology*
University of Patras, 26504 Patras, Greece
[3]*Mechanical Engineering Department*
Technological-Educational Institute of Western Greece
26334 Patras, Greece

Received: 29/12/2013
Accepted: 13/03/2014
Available online: 20/03/2014

*to whom all correspondence should be addressed:
e-mail: estathatos@teipat.gr

ABSTRACT

Tubular halloysite clay mineral and nanocrystalline TiO_2 were incorporated in the preparation of nanocomposite films on glass substrates via sol-gel method at 450 °C. The synthesis involves a simple chemical method employing nonionic surfactant molecule as pore directing agent along with the acetic acid-based sol-gel route without addition of water molecules. Drying and thermal treatment of composite films ensure elimination of organic material and lead to the formation of TiO_2 nanoparticles homogeneously distributed on the surface of the halloysite. Nanocomposite films without cracks of active anatase crystal phase and small crystallite size on halloysite nanotubes are characterized by microscopy techniques and porosimetry methods in order to examine their structural properties. The composite halloysite-TiO_2 films with variable quantities of halloysite were examined as photocatalysts to the discoloration of Basic Blue 41 azo dye in water. These nanocomposite films proved to be very promising photocatalysts and highly effective to dye's discoloration in spite of small amount of halloysite/TiO_2 catalyst immobilized onto glass substrates. It also has been shown that the efficiency of the halloysite/TiO_2 films could be further improved when silver particles were deposited on their surface after successful adsorption from an aqueous solution of a silver salt and UV reduction of the adsorbed ions.

Keywords: Titanium dioxide; nanocrystalline; clay mineral; Halloysite; Photocatalysis; AOPs, Silver modification.

1. Introduction

Wastewater treatment is considered to be a procedure with outmost environmental implications, especially, in the case of industrial wastes. Disposition of colored effluents by textile, paper pulp and other related industries represents a technological issue affecting several countries around the world. In particular,

Rapsomanikis A., Papoulis D., Panagiotaras D., Kaplani E. And Stathatos E., Nanocrystalline TiO_2 and halloysite clay mineral composite films prepared by sol-gel method: Synergistic effect and the case of silver modification to the photocatalytic degradation of basic Blue- 41 azo dye In Water, Global NEST Journal, **16**(3), 485-498.

wastewater pollution from textile industry is one of the major sources of environmental pollution introducing intense coloring and toxicity to the aquatic system. Azo dyes are synthetic colors that contain an azo group, -N=N-, as part of their structure. These dyes account for approximately 60-70% of all dyes used in food and textile manufacture. Most of the azo dyes are chemically stable and are common constituents of effluents in textile industries which demand an appropriate method to dispose them off. The removal of these azo dyes from effluents is difficult since, they are stable to light, heat and oxidizing agents (Robinson *et al.*, 2001; Pearce *et al.*, 2003). Advanced Oxidation Technologies (AOTs) are considered as alternative methods to the decontamination of polluted water. Basically, AOTs are highly efficient treatments to remove recalcitrant dyes from water based on the oxidative power of radical species created during these processes. Photocatalysis as a method belonging to AOTs, is one of the strategies that can be successfully applied to the oxidation and final removal of azo dyes to the formation of carbon dioxide as a latter product. Photodegradation of various organic pollutants by photocatalysis, using wide band gap semiconductors under UV or solar light, has been extensively studied (Chong *et al.*, 2010; Choi *et al.*, 2010; Ahmed *et al.*, 2010). Among them, TiO_2 is a relatively inexpensive semiconductor which exhibits high photocatalytic activity, non-toxicity and stability in aqueous solutions, (Litter, 1999; Song *et al.*, 2009) etc. Furthermore, the synthesis of mesoporous nanocrystalline anatase TiO_2 particles, films or membranes has extended their use in environmental remediation (Choi *et al.*, 2007). Ultra fine TiO_2 powders with high particle surface area have good photocatalytic activity since reactions take place on the surface of the nanocatalyst. On the other hand, powders can easily agglomerate in larger particles and as a consequence adverse phenomena to their photocatalytic activity are observed. Nevertheless, TiO_2 powders cannot easily be recovered from aquatic systems when they are used for water treatment. Highly dispersed TiO_2 particles in suspension are difficult to handle and remove after their application in water and wastewater treatment. However, TiO_2 can also be used as mobilized catalyst exhibiting high catalytic surface area and activity (Choi *et al.*, 2006). Many research studies have been carried out to immobilize TiO_2 catalyst onto various substrates as thin films and membranes. Despite of their lower catalytic surface area compared to powder, significant catalytic activity and utilization have been monitored expanding in this way the field of applications (Bizarro *et al.*, 2009; Sakkas *et al.*, 2010; Li e*t al.*, 2008). The specific surface area, particle morphology and possible aggregation, phase composition and number of -OH surface groups are among the most critical parameters for high photocatalytic activity of the as-prepared films. Another approach to enhance the photocatalytic properties of the catalysts is the promotion of their porous structures.

Several procedures have been applied to the immobilization of TiO_2 with enhanced properties and photocatalytic activity. Glass slides and fibers, membranes, activated carbon and zeolites are used as supports for TiO_2 particles (Wang *et al.*, 2009; Rose *et al.*, 2009; Wang *et al.*, 2008). The efficiency of photocatalytic procedure is generally decreases with catalyst immobilization as the illuminated total surface area is lower than the case of pure TiO_2 powder. However, the use of highly porous materials such as clay minerals can be considered as alternative substrates for TiO_2 immobilized particles (Bouna *et al.*, 2011; An *et al.*, 2008). Halloysite clay mineral with tubular structure could be considered as suitable and also cheap material for TiO_2 particles immobilization (Papoulis *et al.*, 2010; Papoulis *et al.*, 2014). In this work we present the fabrication of thin mesoporous nanocrystalline TiO_2 films in presence of halloysite. The formation of the mesoporosity of the films ought to a template technique based on the sol-gel method with surfactant molecules. The enhanced photocatalytic activity of TiO_2 nanoparticles in combination with halloysite nanocomposite tubes was examined to the discoloration of azo-dye Basic Blue 41 in aqueous solutions. The synergistic effect between TiO_2 and clay mineral tubes was also examined in spite of small amount of TiO_2 catalyst immobilized onto glass substrate. Moreover, we modified the as-prepared composite films with silver in order to increase the photocatalytic efficiency of the films. To the best of our knowledge, it is the first time that halloysite/TiO_2 nanocomposite photocatalysts immobilized on glass substrates with or without the co-existence of silver particles are referred to the decomposition of azo dyes in water.

2. Experimental

2.1. Chemicals and Materials

Pure and well crystalline halloysite samples with tubular morphology were originated from Utah, USA and they were size fractionated by gravity sedimentation to obtain sizes less than 2 μm. Separation of the clay fraction was carried out by using centrifugation methods. The clay fractions of the most halloysite-rich samples were used for the preparation of TiO_2–halloysite nanocomposites. Commercially available Triton X-100 (X100, polyethylene glycol tert-octylphenyl ether), titanium tetraisopropoxide (TTIP), acetic acid (AcOH), Basic Blue 41 (BB-41), silver nitrate (>99%) and all solvents were purchased from Sigma-Aldrich. Double distilled water with resistivity 18.2 MΩ (Millipore) was used in all experiments.

2.2. Sol synthesis

The X100 as a nonionic long chain surfactant organic molecule was selected as a pore directing agent in a sol. Such amphiphilic molecules may succeed the existence of ordered mesophase and the ability to adjust large inorganic clusters in aqueous condition at the same time. A suitable amount of X100 was homogeneously dissolved in ethanol (EtOH). Before adding alkoxide precursor, AcOH was added into the solution for the esterification reaction with EtOH. Then, TiO_2 precursor, TTIP was added at a time under vigorous stirring. The molar ratio of the materials was optimized at X100:EtOH:AcOH:TTIP = 1:69:6:1 in accordance to previous published results (Stathatos *et al.,* 2004). Halloysite (HAL) powder was mixed with previous solution in various quantities following HAL 5%, 20%, 25% and 30% weight ratio compared to TiO_2. After several minutes, the dispersion was ready to be used on glass slides. Films prepared on glass slides for the four HAL weight ratios will be referred as HAL5, HAL20, HAL25 and HAL30 respectively while HAL0 represents pure TiO_2 films without the presence of halloysite.

2.3 Formation of HAL-TiO_2 Thin Films and powders. Silver modification

Borosilicate glass with a size of L75 mm (effective L60) × W25 mm × T1 mm was used as a substrate for fabricating immobilized HAL/TiO_2 thin films. Before coating, the substrate was thoroughly cleaned with detergent and washed with water and acetone and finally dried in a stream of nitrogen. A home-made dip-coating apparatus equipped with a speed controller to maintain a withdrawal rate of ~10 cm min^{-1} was used to dip in and pull out the substrate from the sol. After coating, the films were dried at room temperature for 1 hr, calcined in a multi-segment programmable furnace (PLF 110/30, Protherm) at a ramp rate of 5 °C min^{-1} to 450 °C for 15 min, and cooled down naturally. Only one layer of catalyst was formed for all HAL/TiO_2 ratios. In the case that powders of the above mentioned samples were prepared, the solutions were put in rotary evaporator in order to remove the solvent. Then the viscous sols were heat-treated for 2 hours at 450 °C instead of 15 min as in making thin films in order to remove all the organic content. In this case the heating ramp rate was 1 °C min^{-1}. In case that the as resulted films was chosen to be modified with silver, they were immersed in 1mM silver nitrate aqueous solution. The films were remained in the sol for 15 minutes and then they were rinsed with double distilled water and dried under nitrogen gas. Afterwards, they were exposed to black light (UV source) for 20 minutes while their color was turned to brown which means that adsorbed silver ions were reduced and they were converted to zero valence silver.

2.4. Materials characterization

A Bruker D8 Advance diffractometer with CuKα (λ = 1.5406 Å) radiation and Bragg-Brentano geometry was employed for X-ray diffraction (XRD) studies of the halloysite-TiO_2 catalyst. Nitrogen intrusion/extrusion curves were measured with a Micromeritics Tristar 3000 and the surface area, porosity, and pore size distribution were derived by differentiating them according to BET method. The values were obtained from thick films after scratching the material due to the difficulty of sample collection from the thin films. For the

visual morphology of HAL/TiO_2 nanostructure, an environmental scanning electron microscope (FESEM, Zeiss SUPRA 35VP) was used and inspect film homogeneity. Absorption measurements of BB-41 sols were carried out with a Hitachi U-2900 UV-Vis spectrophotometer.

2.5 Photocatalytic activity of HAL-TiO_2 composite films

A cylindrical reactor presented in a previous publication (Stathatos *et al.,* 2012) was used in all experiments. Air was pumped through a gas inlet using a small pump to ensure continuous oxygen supply to the reaction solution while simultaneously agitating it. Four Black lights with 4 W nominal power were placed around the reactor for UV illumination. The whole construction was covered with a cylindrical aluminum reflector. Cooling was achieved by air flow from below the reactor using a ventilator. The catalyst was in the form of four borosilicate glasses, covered on one side with nanocrystalline HAL%-TiO_2 films. The total surface of the photocatalyst films was approximately 60 cm^2 while the catalyst mass was approximately 50 mg. The reactor was filled with 80 ml of $2.5x10^{-5}$ mol l^{-1} BB-41 aqueous solution. This dye is strongly adsorbed on pure or halloysite modified TiO_2 films. For this reason, we stored the solution in the presence of the photocatalyst in the dark for an hour and all of our photocatalytic results were obtained after equilibrium. The photocatalytic discoloration process for the dye was examined by monitoring the absorption maximum of the BB-41 solution (610 nm) at various irradiation times. Photocatalytic discoloration rate of BB-41 was calculated by the formula

$$r=\frac{C_o-C}{C_0}$$

as the concentration of the dye is proportional to the absorbance for low concentration values. Where C_0 is the initial concentration of BB-41 solution and C is the final concentration after irradiation with UV light. Discoloration efficiency is determined as

$$eff\%=\frac{C_o-C}{C_0}100\%$$

For repeated use of the photocatalysts, the films were washed with distilled water and dried at 80 °C while no further treatment was followed for the films.

3. Results and discussion

3.1. Structural properties of HAL-TiO_2 nanocomposites

Composite halloysite-TiO_2 films prepared on borosilicate glass substrates for different HAL weight proportions as described in experimental section. Samples, abbreviated as HAL5, HAL20, HAL25 and HAL30 represent different weight proportions of halloysite in TiO_2 sol while HAL0 is referred to pure TiO_2. After calcination at relatively high temperature (450 °C) for removing the organic template all films were firmly attached on the glass because of TiO_2 without any cracks. Halloysite was finely dispersed in the films for any proportion was used. First, the crystallinity of the films was examined in order to detect any differences to the crystal structure of halloysite after heating and the crystal phase of resulting nanocomposite TiO_2. The XRD patterns of all films are presented in Fig.1. Strong reflection at $2\theta=12.2^0$ is corresponded to halloysite 7Å, while a less intensive reflection at 2θ equal to 8.80^0 corresponds to halloysite 10Å (Fig.1, curve a). The main peak of halloysite 7Å seems that is remaining after heating but it is much lower mainly to the low amount of the mineral in films proving the remaining crystallinity of the clay mineral. A second reason is probably the partial dehydration of halloysite due to the temperature applied for the synthesis of the films. It should be noted that in this sample (Fig.1, curve a) low amounts of quartz are also present (main reflections observed at 26.60^0 and 20.80^0).

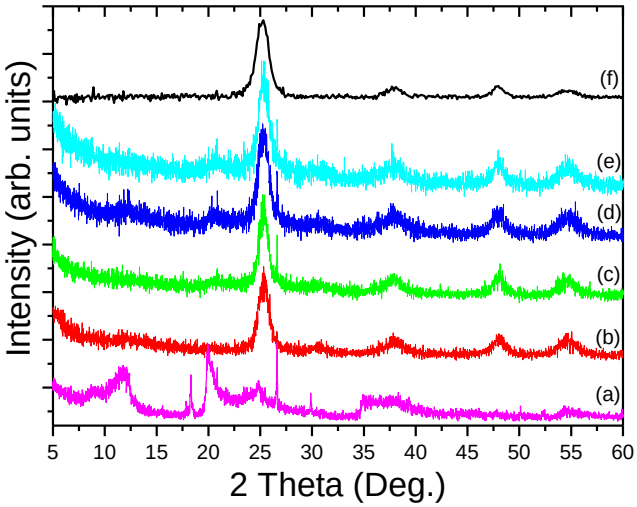

Figure 1. XRD patterns of Halloysite-TiO_2 nanocrystalline films:
(a) powder of halloysite clay mineral as a reference (b) HAL5, (c) HAL20, (d) HAL25, (e) HAL30, (f) HAL0

Titania pure nanocrystalline film (HAL0) is also presented in Fig.1 (curve f) where a reflection (101) of anatase form at $2\theta=25.1^0$ is observed. The two basic reflections at $2\theta=12.2^0$ and $2\theta=25.1^0$ for HAL and TiO_2 are maintained at the rest of samples with different intensity ratio because of the variable proportion between them. The grain size for TiO_2 has been calculated from XRD patterns using Scherrer's equation: $D=0.9\lambda/(s\cos\theta)$, where λ is the wavelength of the X-ray and s is the full width (radians) at half maximum (FWHM) of the signal. The crystallite size for TiO_2 is calculated 7.5, 8.1, 11.3, 8.5 and 9.4 nm for samples HAL0, HAL5, HAL20, HAL25 and HAL30 respectively.

Table 1. Structural characteristics of Halloysite-TiO_2 films

Sample	Total pore volume Vp ($cm^3\ g^{-1}$)	Specific surface area S ($m^2\ g^{-1}$)	Total porosity φ(%)	Mean pore diameter D_{por} (nm)
Halloysite	0.125	50.9	24.46	9.85
TiO_2 (HAL0)	0.133	121.3	33.58	4.78
5% Hal-TiO_2 (HAL5)	0.165	108.6	39.10	6.09
20% Hal-TiO_2 (HAL20)	0.155	77.5	37.62	7.98
25% Hal-TiO_2 (HAL25)	0.171	95.3	39.95	7.20
30% Hal-TiO_2 (HAL30)	0.159	106.2	38.21	6.01

All the peaks indicated that the crystal phase of the materials containing TiO_2 was anatase and the relatively large width of peaks indicated that the size of the nanocrystallite was less than 12 nm. It should be noted that it is evident from the XRD patterns that the calcination at 450 °C for 15 min did not completely destroy halloysite.

Because of the difficulty in directly characterizing the porosity of immobilized HAL-TiO_2 thin films, the characterizations were carried out on the corresponding particles. The structural characteristics of HAL-TiO_2 particles are shown in Table 1.

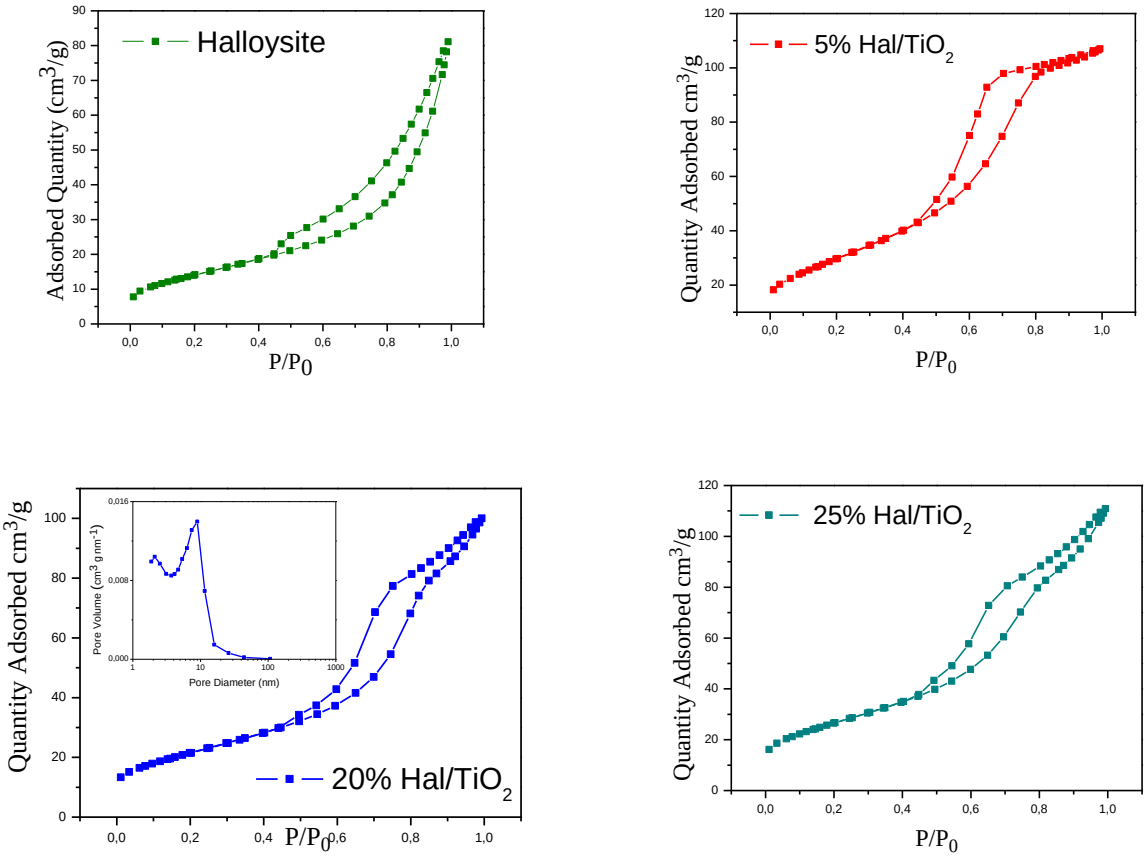

Figure 2. Sorption-desorption isotherms and pore size distribution (20% in Halloysite) for several %wt of Halloysite in composite Halloysite-TiO_2 material

The specific surface area S, the total pore volume V_p, the mean pore diameter D_{por}, and the total porosity ϕ were calculated for all samples and they are presented in Table 1.

Pure halloysite has relatively large pore volume while similar result was obtained for pure TiO_2. On the other hand their mixtures possess slightly greater values. As it concerns the particle surface areas, in the case of pureTiO_2 a relatively high value of 121.3 m^2 g^{-1} is measured and 50.9 m^2 g^{-1} for halloysite. All other samples with different proportions of halloysite in TiO_2 matrix exhibit intermediate values for particle surface areas as they appear in Table 1. The nitrogen sorption-desorption curves of samples HAL5, HAL20 and HAL25 are presented in Fig.2 and the pore size distribution for HAL20 as an example appear as an inset of Fig.2b. This porosity is, also, apparent in SEM images shown in Fig.3. Halloysite samples are consisted of tubular particles as it can be seen in Fig.3a. The average diameter of the tubes, as they were observed before modification, is 40-70nm while the length is between 100-500nm. After modification, TiO_2 nanoparticles uniform in size overlay halloysite tubes.

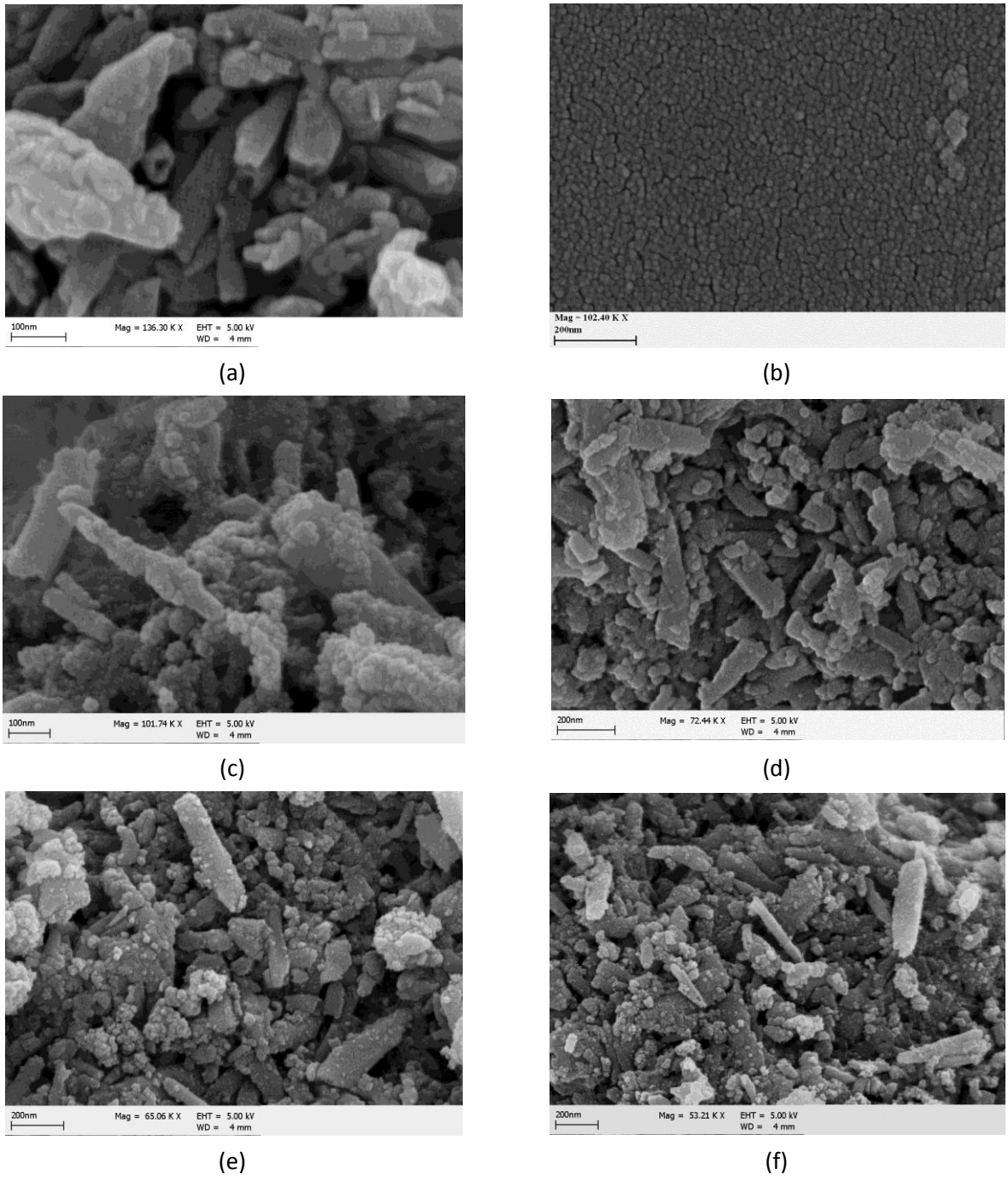

Figure 3. SEM images of: (a) Halloysite powder, (b) pure TiO_2, (c) HAL5, (d) HAL20, (e) HAL25 and (f) HAL30 films

Besides, TiO_2 nanoparticles help to the stabilization of the composite material on the borosilicate glass substrate after calcination by forming stable Ti-O-Si bonds (Stathatos *et al.,* 1997; Liu, 1999). In Fig.3c, d, e and f halloysite nanotubes seem to be completely covered with uniform layers of TiO_2 and uniform particle distribution. The thickness of TiO_2 film without halloysite tubular particles is around 180-200 nm with only

one dipping layer according to cross sectional SEM image. The homogeneity of TiO_2 particles' size and film can be seen in all images of Fig.3. According to images of Fig.3 the TiO_2 crystal grains have a spherical shape while they have an average size ranging from 12 to 16 nm. TiO_2 particles were also found to form aggregates on halloysite external surfaces but these were of uniform small size as it was also proved by porosimetry data. The dispersion of halloysite in TiO_2 films is obvious but it is firmly agglutinated. No cracks or peeling off traces around halloysite boundaries were observed. The film is permanently attached on the glass substrate with good adherence while halloysite cannot be rived from the composite material. The evidences of SEM images for the nanocomposite material may help us to schematic represent the film fabrication on glass substrates (scheme 1). It is assumed that the organophilic interphase, assured by X100 surfactant coating, acts like a templating medium which provides titanium dioxide nanoparticles with relatively monodispersed particle sizes on the surface. The initially amorphous TiO_2 phase was crystallized after calcination at 450^0C for 15 min in air while X100 was completely burned out.

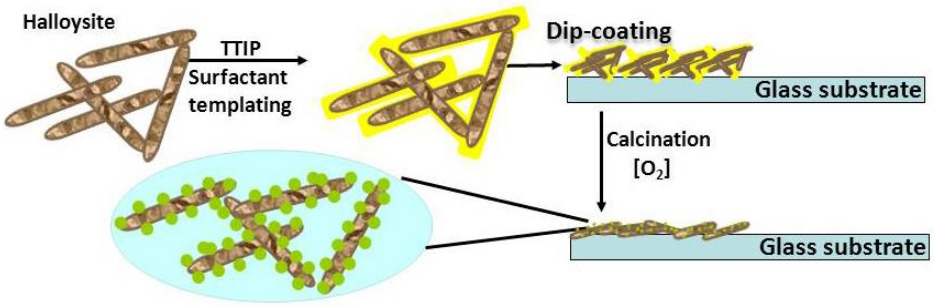

Scheme 1. Procedure of HAL-TiO_2 nanocomposite photocatalyst formation as films after calcination to promote TiO_2 nanoparticles

Silanol groups (Si-OH) of clay mineral can react with titanium alkoxide giving covalently bonded organic-inorganic derivatives, which could be useful for anchoring metal oxide nanoparticles on halloysite surface. From the SEM observations it is evident that halloysite tubes were not destroyed from the temperature involved in the synthesis.

3.2. Photocatalytic activity of composite halloysite and TiO_2 films

It is commonly known that titanium dioxide mediated photo-degradation involves the generation of electron-hole pairs (Litter, 1999), which migrate to the photocatalyst surface forming surface bound hydroxyl and superoxide radicals according to following equations:

$$TiO_2 + h\nu \rightarrow e^-_{cb} + h^+_{vb}$$

$$O_2 + e^-_{cb} \rightarrow O_2^{-\bullet}$$

$$H_2O + h^+_{vb} \rightarrow {}^{\bullet}OH + H^+$$

It is also commonly known that the hydroxyl and superoxide radicals are the primary oxidizing species in the photocatalytic process. These oxidative reactions result in the photodiscoloration of dyes as target pollutants in water. Photocatalytic experiments were undertaken on Basic Blue 41 to evaluate HAL-TiO_2 composite catalyst in films as shown in Fig. 4. The different weight percentages of halloysite in TiO_2 nanocrystalline films showed slight variations to the photocatalytic activities of the films. The rate of discolorization was monitored with respect to the change in intensity with time of the absorption peak at 610 nm. The absorption peak of the dye diminished with time and disappeared during the reaction indicating that it had been decomposed. Besides, the UV illumination was started after one hour of the photocatalyst presence in dye's sol in order to be in equilibrium before illumination. The results also show

that there was no direct photolysis of BB-41 in the absence of any photocatalyst. In the case of HAL20 a complete decolorization was reached within 140 min of illumination implied the synergistic effect between clay mineral and TiO_2 by preparing highly porous HAL-TiO_2 catalysts. However, the further addition of halloysite in films caused a slight decrease on the photocatalytic activity of films mainly at early stage of the procedure. The combination of clay mineral porous structure with uniform coverage of TiO_2 particles on the surface could provide more active sites for dye stuff discoloration. This is also proved by the higher values measured for the porosity and mean pore diameter of the composite HAL-TiO_2 compared to the pure TiO_2 and Halloysite. However, we may not guarantee that dipping procedure for the film formation succeeds a clear discrimination concerning the quantity of halloysite in films with variable HAL-TiO2 percentage when the clay mineral is dispersed in high amounts in the sol. So, an error to the experimental data presented in Figure 4 cannot be excluded and we estimate it to be at the level of 2-3%.

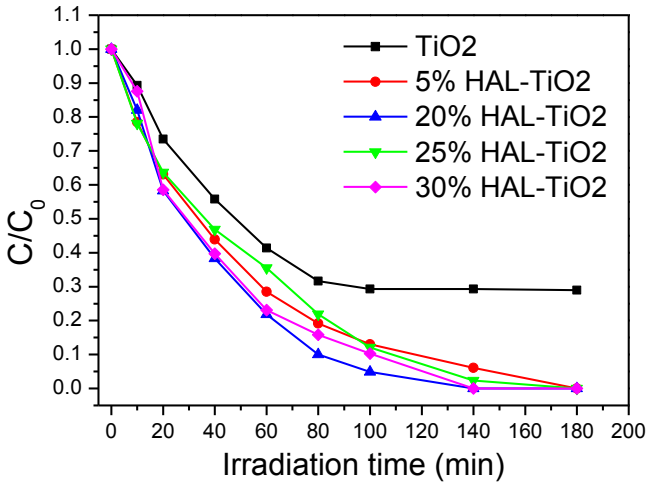

Figure 4. Photo-discoloration of BB-41 by TiO_2 films in presence of different weight percentages of halloysite under UV light

Considering the small amount of TiO_2 catalyst immobilized onto the substrate, the HAL-TiO_2 films were highly efficient to degrade the azo dye. As a consequence, the tubular nanocomposite materials can be an alternative substrate for the growth of nanoparticle TiO_2 achieving an efficient photocatalyst. Decomposition kinetics of BB-41 has been observed to follow first-order kinetics and it is well established that photo-discoloration experiments follow Langmuir-Hinshelwood model, where the reaction rate, r, is proportional to the surface coverage, θ, according to the following equation (Ibhadon *et al.,* 2008):

$$r=-\frac{dC}{dt}=k_1\vartheta=\frac{k_1KC}{1+KC} \quad (1)$$

where k_1 is the reaction rate constant, K is the adsorption coefficient of the reactant and C is the reactant concentration. In the case that C is very small, KC factor is negligible in respect to unity and the equation (1) describes first-order kinetics. The integration of eq.1 yields to the eq.2:

$$-\ln\left(\frac{C}{C_o}\right)=k_{app}t \quad (2)$$

With limit condition that on t=0 we have the initial concentration C_0. k_{app} is the apparent first-order rate constant. Discoloration kinetics of BB-41 in presence of different HAL proportions in TiO_2 nanocrystalline

films is presented in Fig.5. The maximum value for rate constant was calculated for sample HAL20 ($29.8x10^{-3}$ min^{-1}) while the value for pure TiO_2 film was estimated at $12.9x10^{-3}$ min^{-1} (Table 2). Furthermore, all the samples HAL-TiO_2 exhibited better performance than pure TiO_2. We mainly attribute this behavior to the internal light scattering because of the presence of the halloysite. The poor photocatalytic performance observed for pure TiO_2 films after 100 min of irradiation is mainly due to the limited quantity of the material as the total thickness of the films was approximately 180nm (1 layer of TiO_2). However, the composite HAL-TiO_2 material with only one layer has substantial performance compared to pure TiO_2 which proves the effectiveness of the halloysite presence in the films.

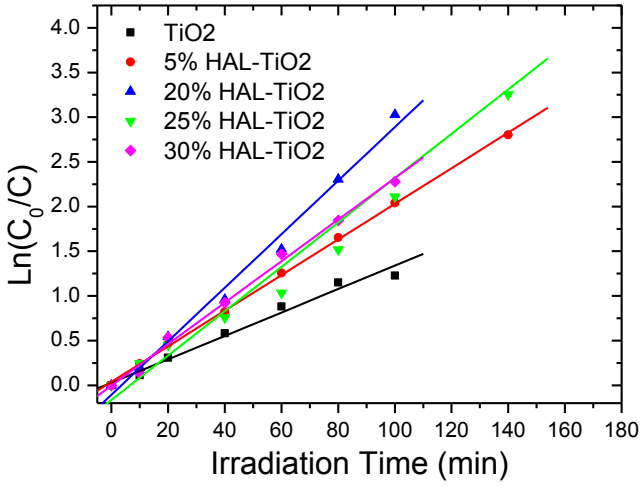

Figure 5. Ln(C_0/C) as a function of irradiation time for HAL-TiO_2 photocatalysts

This is also could be attributed to better structural characteristics of the films compared to pure TiO_2 film mainly tabulated at porosity and total pore volume. However, the rate of dye discolorization depends on adsorption of the dye into the catalyst porous structure. Finally, it has been found that the same photocatalysts can be used in several photocatalytic cycles without remarkable loss to their efficiency.

Table 2. Constant of BB-41 degradation rate in the presence of Halloysite-TiO_2 composite films modified with silver particles

Sample	k_{app} ($x10^{-3}$ min^{-1})	k_{app} ($x10^{-3}$ min^{-1})
	w/o silver	*with silver*
0% Hal-TiO_2	12.9	18.5
5% Hal-TiO_2	19.8	19.8
20% Hal-TiO_2	29.8	26.6
25% Hal-TiO_2	24.8	25.3
30% Hal-TiO_2	23.2	28.5

3.3. Photocatalytic activity of silver modified halloysite-TiO_2 films

As an alternative procedure to further increase the efficiency of the HAL-TiO_2 photocatalysts silver ions were deposited on the TiO_2 surface by submerging TiO_2 films in aqueous solutions of metal salt for several minutes. It generally believed that silver modified TiO_2 could cause a better separation of charge carriers on the oxide surface (Stathatos *et al.,* 2000). Metal cations could be adsorbed onto TiO_2 films at substantial

quantities because of the relatively high specific surface area of the films. In the case of silver ions and after their adsorption only one electron is enough to reduce silver ions and create zero valence noble metal on the surface of TiO_2, according to the following equation:

$$Ag^{+1} + e^{-} \rightarrow Ag^{0}$$

This electron is easy to be generated, either by UV illumination under black light irradiation or by thermal heating of the films (Stathatos *et al.,* 2000).

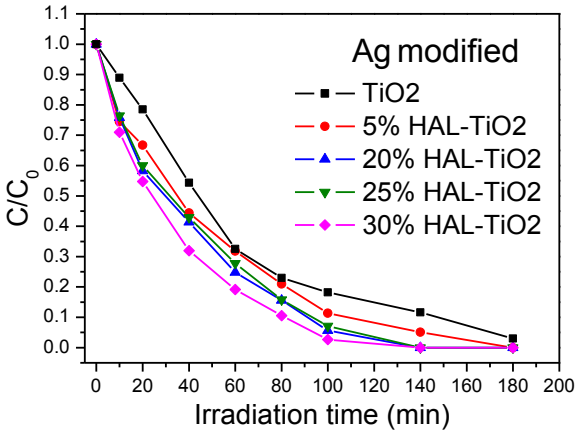

Figure 6. Photo-discoloration of BB-41 by silver particles modified TiO_2 films in presence of different weight percentages of halloysite under UV light

Indeed, the films after UV exposure were turned to light brownish colored attributed to the creation of zero valence silver due to plasmon resonance absorption (Gong *et al.,* 2012). The corresponding photocatalytic experiments to evaluate the silver modified HAL-TiO_2 composite catalyst in films are shown in Fig. 6. However, the original salt concentration obviously affects the quantity of deposited metal, affected photo-discoloration efficiency. When the silver salt concentration was 10^{-3} mol l^{-1} we obtained the highest photocatalytic efficiency.

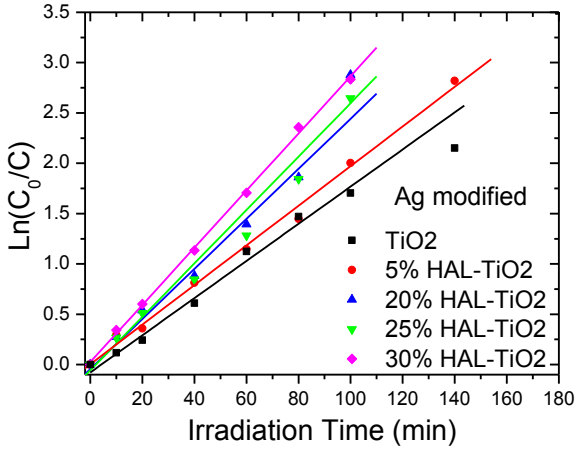

Figure 7. $\ln(C_0/C)$ as a function of irradiation time for silver modified HAL-TiO_2 photocatalytic films

At higher metal load, efficiency dropped, possibly due to screening effects. Decomposition kinetics of BB-41 in presence of silver modified HAL-TiO_2 films, have been observed to follow first-order kinetics as in the case of bare HAL-TiO_2 films. The data are presented in Table 2 and Fig.7.

In the case of silver modification the most efficient films are proved to be HAL30 where a complete discoloration of the dye was achieved within 100 minutes.

For a direct comparison among HAL-TiO2 films and silver modified ones to the photocatalytic decomposition of BB-41, we present the data of Fig.8.

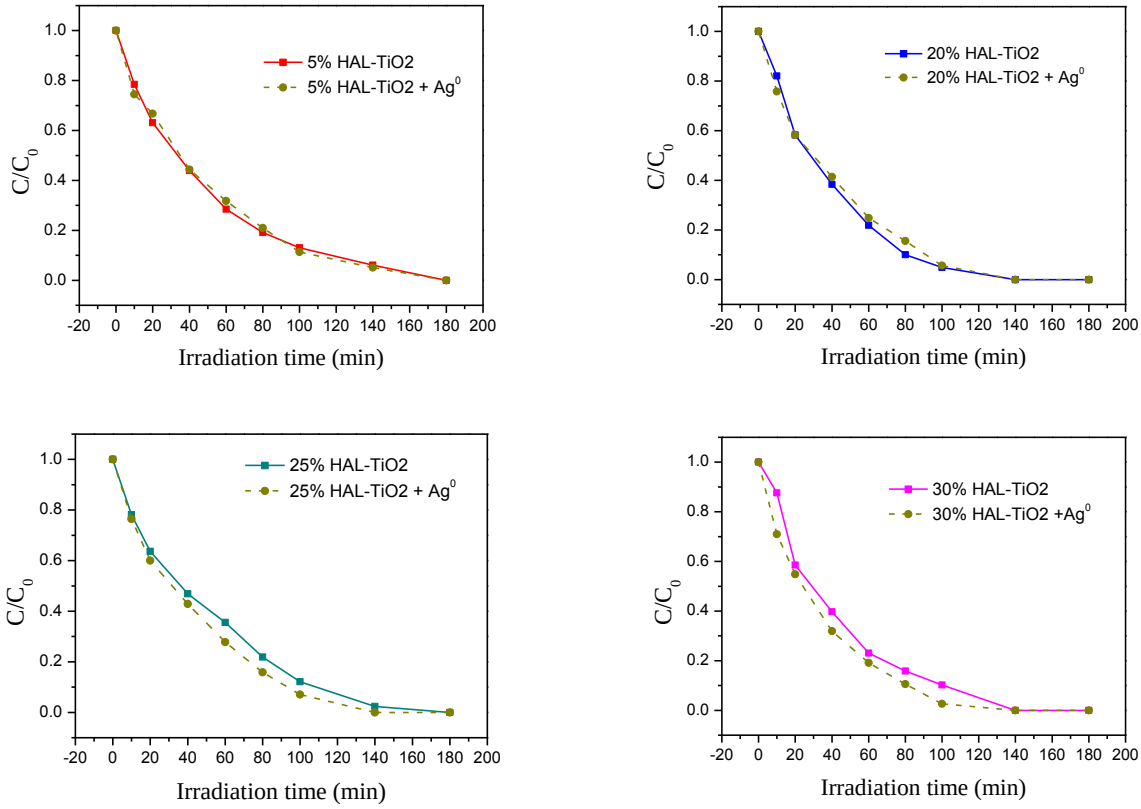

Figure 8. Comparison between bare and silver modified HAL-TiO_2 films to the photo-discoloration of BB-41

It is obvious that silver modified films exhibit a slight better performance to the discoloration of BB-41 mainly due to the better separation of charge carriers on the oxide surface. Further experiments with several noble metals modified composite HAL-TiO_2 films are under way.

4. Conclusions

Highly porous nanostructured HAL-TiO_2 particles and films were synthesized via sol-gel method composed of ethanol, acetic acid, titanium tetraisopropoxide, halloysite nanotubes and nonionic surfactant molecules as organic template. Slow hydrolysis reaction and stable incorporation of inorganic network onto surfactant molecules made it possible to control the subsequent porous nanostructure. The HAL-TiO_2 films exhibited enhanced structural properties including crystallinity and active anatase phase while enhanced photocatalytic properties to the discoloration of BB-41 in water were succeeded. The experiments on photocatalytic discoloration of BB-41 implied the importance of synergistic effect between clay mineral

nanotubes and TiO_2 nanoparticles. In addition, the presence of silver particles on the surface of the composite photocatalyst could further increase the efficiency of the catalyst due to better separation of charge carriers on the TiO_2.

Acknowledgement

The authors would like to acknowledge financial support from the European Union (Lead Market European Research Area Network - LEAD ERA) and the Regional Authority of Western Greece under the project "INDOOR ECOPAVING". The project is implemented under the Operational Program "DEPIN 2007-2013" Priority Axis (PA) 'Digital convergence and entrepreneurship in Western Greece', action "Transnational Business Collaboration Western Greece" and is co-funded by the European Union –European Regional Development Fund and National Resources (NSRF 2007-2013). Besides, the authors are thankful to Dr. V. Dracopoulos, FORTH/ICE-HT, for his help to the FE-SEM images.

References

Ahmed S., Rasul M.G., Martens W.N., Brown R. and Hashib M.A. (2010), Heterogeneous photocatalytic degradation of phenols in wastewater: A review on current status and developments, *Desalination*, **261**, 3-18.

An T., Chen J., Li G., Ding X., Sheng G., Fu J., Mai B. and O'Shea K.E. (2008), Characterization and the photocatalytic activity of TiO_2 immobilized hydrophobic montmorillonite photocatalysts: Degradation of decabromodiphenyl ether (BDE 209), *Catalysis Today*, **139**, 69-76.

Bizarro M., Tapia-Rodríguez M.A., Ojeda M.L., Alonso J.C. and Ortiz A. (2009), Photocatalytic activity enhancement of TiO_2 films by micro and nano-structured surface modification. *Applied Surface Science*, **255**, 6274-6278.

Bouna L., Rhouta B., Amjoud M., Maury F., Lafont M.-C., Jada A., Senocq F. and Daoudi L. (2011), Synthesis, characterization and photocatalytic activity of TiO_2 supported natural palygorskite microfibers, *Applied Clay Science*, **52**, 301-311.

Choi H., Al-Abed S.R., Dionysiou D.D., Stathatos E. and Lianos P. (2010), Chapter 8 TiO_2-Based Advanced Oxidation Nanotechnologies for Water Purification and Reuse, *Sustainability Science and Engineering*, **2**, 229-254, Elsevier.

Choi H., Stathatos E. and Dionysiou D.D. (2006), Sol–gel preparation of mesoporous photocatalytic TiO_2 films and TiO_2/Al_2O_3 composite membranes for environmental applications, *Applied Catalysis B: Environmental*, **63**, 60-67.

Choi H., Stathatos E. and Dionysiou D.D. (2007), Photocatalytic TiO_2 films and membranes for the development of efficient wastewater treatment and reuse systems, *Desalination*, **202**, 199-206.

Chong M.N., Jin B., Chow C.W.K. and Saint C. (2010), Recent developments in photocatalytic water treatment technology: A review, *Water Research*, **44**, 2997-3027.

Gong D., Chye W., Ho J., Tang Y., Tay Q., Lai Y., Highfield J.G. and Chen Z. (2012), Silver decorated titanate/titania nanostructures for efficient solar driven photocatalysis, *Journal of Solid State Chemistry*, **189**, 117-122.

Ibhadon A.O., Greenway G.M., Yue Y., Falaras P. and Tsoukleris D. (2008), The photocatalytic activity and kinetics of the degradation of an anionic azo-dye in a UV irradiated porous titania foam, *Applied Catalysis B: Environmental,* **84**, 351-355.

Li F., Sun S., Jiang Y., Xia M., Sun M. and Xue B. (2008), Photodegradation of an azo dye using immobilized nanoparticles of TiO_2 supported by natural porous mineral, *Journal of Hazardous Materials*, **152**, 1037-1044.

Litter M.I. (1999), Heterogeneous photocatalysis: Transition metal ions in photocatalytic systems, *Applied Catalysis B: Environmental*, **23**, 89-114.

Liu J.-C. (1999), M_x-O_y-Si_z Bonding Models for Silica-Supported Ziegler-Natta Catalysts, *Appl. Organometal. Chem.*, **13**, 295–302.

Papoulis D., Komarneni S., Nikolopoulou A., Tsolis-Katagas P., Panagiotaras D., Kacandes H.G., Zhang P., Yin S., Sato T. and Katsuki H. (2010), Palygorskite- and Halloysite-TiO_2 nanocomposites: Synthesis and photocatalytic activity, *Applied Clay Science*, **50**, 118-124.

Papoulis D., Komarneni S., Panagiotaras D., Stathatos E., Christoforidis K.C., Fernández-García M., Li H., Shu Y., Sato T. and Katsuki H. (2014), Three-phase nanocomposites of two nanoclays and TiO_2: Synthesis, characterization and photacatalytic activities, *Applied Catalysis B: Environmental*, **147**, 526-533.

Pearce C.I., Lloyd J.R. and Guthrie J.T. (2003), The removal of colour from textile wastewater using whole bacterial cells: a review, *Dyes and Pigments*, **58**, 179-196.

Robinson T., McMullan G., Marchant R. and Nigam P. (2001), Remediation of dyes in textile effluent: a critical review on current treatment technologies with a proposed alternative, *Bioresource Technology*, **77**, 247-255.

Rose G., Echavia M., Matzusawa F. and Negishi N. (2009), Photocatalytic degradation of organophosphate and phosphonoglycine pesticides using TiO_2 immobilized on silica gel, *Chemosphere*, **76**, 595-600.

Sakkas V.A., Islam Md. A, Stalikas C. and Albanis T.A. (2010), Photocatalytic degradation using design of experiments: A review and example of the Congo red degradation, *Journal of Hazardous Materials*, **175**, 33-44.

Song X.-M., Wu J.-M. and Yan M. (2009), Photocatalytic degradation of selected dyes by titania thin films with various nanostructures, *Thin Solid Films*, **517**, 4341-4347.

Stathatos E., Lianos P., Del Monte F., Levy D. and Tsiourvas D. (1997), Formation of TiO_2 nanoparticles in reverse micelles and their deposition as thin films on glass substrates, *Langmuir,* **13**, 4295-4300.

Stathatos E., Lianos P., Falaras P. and Siokou A. (2000), Photocatalytically Deposited Silver Nanoparticles on Mesoporous TiO_2 Films, *Langmuir*, **16**, 2398-2400.

Stathatos E., Lianos P. and Tsakiroglou C. (2004), Highly efficient nanocrystalline titania films made from organic/inorganic nanocomposite gels, *Microporous and Mesoporous Materials*, **75**, 255-260.

Stathatos E., Papoulis D., Aggelopoulos C.A., Panagiotaras D. and Nikolopoulou A. (2012), TiO_2/palygorskite, composite nanocrystalline films prepared by surfactant templating route: Synergistic effect to the photocatalytic degradation of an azo-dye in water, *Journal of Hazardous Materials*, **211–212**, 68-76.

Wang C.-C., Lee C.-K., Lyu M.-D. and Juang L.-C. (2008), Photocatalytic degradation of C.I. Basic Violet 10 using TiO_2 catalysts supported by Y zeolite: An investigation of the effects of operational parameters, *Dyes and Pigments*, **76**, 817-824.

Wang X., Liu Y., Hu Z., Chen Y., Liu W. and Zhao G. (2009), Degradation of methyl orange by composite photocatalysts nano-TiO_2 immobilized on activated carbons of different porosities, *Journal of Hazardous Materials*, **169**, 1061-1067.